

2012-2023 Comparative Ground Penetrating Radar and Temperature Survey at Orakei Korako, Taupō Volcanic Zone, New Zealand

Bridget Lynne^{1,2}, Gary Smith², Isaac Smith²

¹University of Auckland, 70 Symonds St, Auckland, New Zealand

²Geothermal Scientific Investigations Ltd, 11 Kyle Rd, Greenhithe 0632, Auckland, New Zealand

b.lynn@auckland.ac.nz or bridget.lynn@gsilimited.com

Keywords: *Keywords should be listed in Time New Roman, 9pt, italics with a comma separating each.*

ABSTRACT

In 2012, a Ground Penetrating Radar (GPR) and downhole temperature measurement survey was undertaken around the boardwalk at Orakei Korako geothermal field, Taupō Volcanic Zone, New Zealand. In 2023, this survey was repeated to identify if and where changes in the subsurface had taken place over the last 11 years.

Nine 2012 downhole temperature measurement sites and ten surface temperature measurements sites were repeated for a direct comparison with our 2023 data. Downhole temperature measurements were taken where possible at depths of 0.5 m, 1.0 m and 1.5 m using a K-type digital temperature probe with a quick response tip. Surface temperature measurements were obtained at the start and end points of each GPR transects using a digital temperature probe with a K-type thermocouple.

Thirteen GPR sites were repeated in 2023, five 2012 GPR sites were not repeated due to inaccessibility to the site. GPR profiles from seven new sites were also collected during the 2023 survey. In 2012 we used a GSSI SIR-2000 GPR unit with a 200 MHz antenna. In 2023 a Leica DS2000 GPR unit fitted with dual frequency antennae of 250 MHz and 700 MHz was used. The 700 MHz antennae collected high resolution data from the shallow subsurface (0-3 m depth), while the 250 MHz antennae captured data from deeper layers (0-7 m) at a coarser resolution.

Our repeat survey identified areas that have heated up and cooled down, mapped migrating subsurface heat pathways, located ascending steam conduits, identified fractures, mapped zones of hydrothermal alteration, as well as imaged the thickness of the siliceous sinter terraces.

The combined techniques of GPR and temperature measurements offers an innovative method and new perspective for characterising changes that take place in the shallow subsurface over time.

1. INTRODUCTION

Orakei Korako is a protected geothermal system and tourist site located within the Taupō Volcanic Zone (TVZ), New Zealand (Fig. 1). The main thermal area is accessed via a short boat trip across the Waikato River at Lake Ohakuri (Fig. 1). Orakei Korako is privately owned, but open to the public, with well-formed boardwalks and paths around the geothermal field.

Thermal activity is abundant at Orakei Korako and consists of a few acid features such as mud pools, fumaroles and steaming ground, but is dominated by discharging alkali chloride hot springs and pools with expansive siliceous sinter

terraces. Sinters are hot spring rocks formed as silica precipitates and accumulates from discharging alkali chloride hot spring waters (Fournier and Rowe, 1966; Fournier, 1985; Williams and Crerar, 1985). Sinters remain at the surface for thousands of years even after hot spring discharge ceases, providing ground level evidence of an alkali chloride geothermal reservoir at depth (Campbell et al., 2001; Lynne et al., 2005, 2008; Campbell et al, 2015).

Surface thermal activity is sensitive to even subtle changes in hydrology. For example, hot spring flow rates may increase or decrease or cease altogether. A decrease in reservoir pressure can be reflected at the surface by an increase of discharging steam and gases, and a decrease in hot spring flow rate. When ascending steam and hydrogen sulphide gas mix with atmospheric oxygen, acidic steam condensate is formed. Acidic steam condensate descends through the ground and/or sinter, dissolving and/or hydrothermally altering it as it migrates through permeable pathways. This process can take place below the ground surface with no evidence of heat or gas discharge at the surface.

Ground Penetrating Radar (GPR) has proven to be a useful tool to image the shallow subsurface in geothermal settings to <10 m depth. GPR can map the thickness of exposed and buried siliceous sinters (Lynne and Dougherty, 2010a, b; Dougherty and Lynne, 2010a; Foley et al., 2015; Lynne et al., 2016a), the location, orientation and connectivity of subsurface fractures (Dougherty and Lynne, 2010b; Dougherty and Lynne, 2011; Jaworowski et al., 2020), shallow hydrological changes (Lynne et al., 2016b; Lynne et al., 2018) and the occurrence of shallow steam zones and/or intensely hydrothermally altered areas (Lynne et al., 2017). When GPR is combined with downhole temperature measurements, the measured subsurface temperature confirms if hydrothermal alteration is present-day or historic (Lynne and Smith, 2014). The combined techniques of GPR and downhole temperature measurement provide a useful method to track shallow changes in the subsurface over time, and are especially useful for identifying subsurface changes when there is no evidence of heat or change at the surface.

In 2012 we completed a survey around the boardwalk at Orakei Korako where we combined GPR with downhole temperature measurements taken at 0.5 m, 1.0 m and 1.5 m depth. In 2023, this survey was repeated so we could compare the results of the two surveys and identify any changes over the last 11 years.

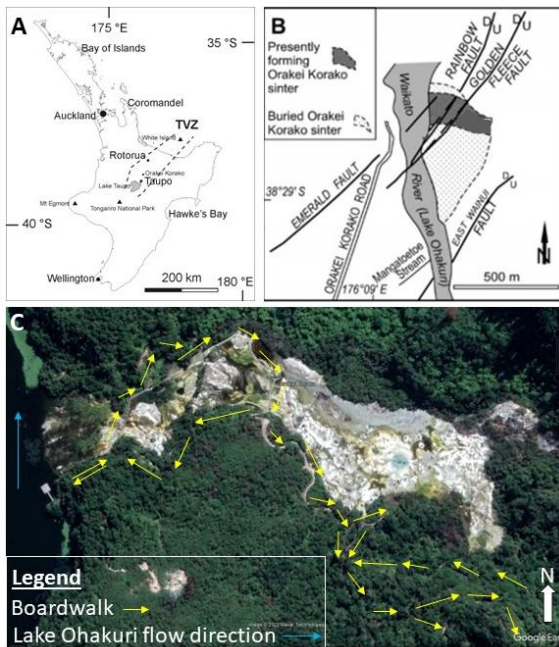


Figure 1: Orakei Korako. (A) Location within the Taupō Volcanic Zone (TVZ), New Zealand. (B) Faults and siliceous sinter terraces at Orakei Korako. (C) Boardwalk around siliceous sinter terraces and bush.

2. METHODS

2.1 Ground Penetrating Radar

In 2012, the GPR unit used was a GSSI SIR-2000 with a GSSI 200 MHz antenna. Data was collected in continuous run mode at 200 ns. Topographic correction was not required as the GPR transects were along level boardwalks and ground surfaces.

In 2023, the GPR unit used was a Leica DS2000 fitted with dual frequency antennas of 250 MHz and 700 MHz. The 700 MHz antennae collected high resolution data from the shallow subsurface (0-3 m depth), while the 250 MHz antennae captured data from deeper layers (0-7 m), at a coarser resolution. At the start of the survey, data was collected using 80 ns, 150 ns and 200 ns, to compare quality of data with respect to depth. After comparison, 150 ns was chosen for this survey as an ideal compromise between depth and image resolution. Data was collected in continuous run mode at 512 samples per scan and 306 scans per metre. Topographic correction was not required for these surveys as the GPR transects were on level surfaces. The air gap between the antenna and the ground surface was removed during data processing. No gain was added during post-processing.

GPR profiles can be presented in colour or grayscale. Our 2012 images are shown in colour while our 2023 images are shown in grayscale. GPR profiles can show high, medium or low amplitude reflections (Fig. 2). The strength of the reflection depends on the dielectric properties of the subsurface rocks, which is influenced by hydrothermal alteration processes and the presence of fluid and air.

Based on our previous GPR studies undertaken in geothermal settings, GPR reflections can be grouped as follows:

- Strong competent unaltered siliceous sinters produce strong, or high amplitude reflections.

- Moderately-altered rocks or siliceous sinters produce medium amplitude reflections.
- Highly-altered rocks, sinters or clays produce weak or low amplitude reflections.
- Fractures appear as offset layers.
- Subsurface steam conduits are imaged as vertical weak amplitude reflections. Elevated measured temperatures confirm present-day heat in the subsurface.
- Hyperbolas are caused when the radar wave reflects off a single point round object, such as buried service pipes.

Our 2012 Orakei Korako GPR and temperature survey was ground-truthed by collecting siliceous sinter samples and analysing them using Scanning Electron Microscopy. Our 2012 survey confirmed that where GPR was collected over unaltered sinter, strong amplitude reflections were detected. Weak amplitude reflections were detected where steam was ascending and hydrothermally altering the sinter (Lynne and Smith, 2014).

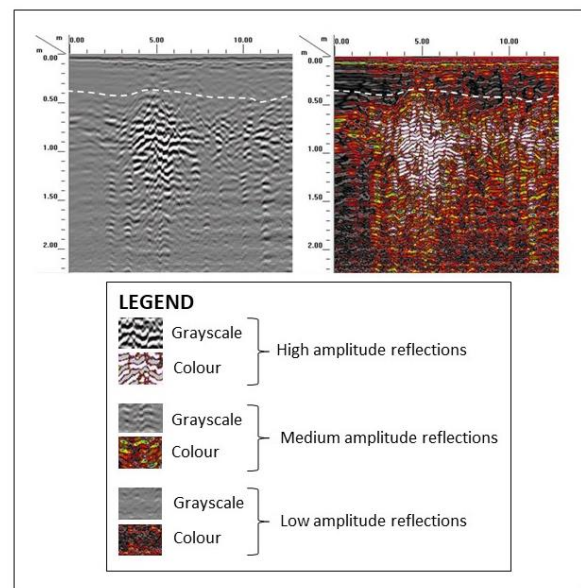


Figure 2: An example of a GPR image showing low, medium and high amplitude reflections, typical of those imaged at Orakei Korako.

2.2 Temperature Measurements

Two sets of temperature measurements were collected for these surveys: (1) Downhole temperature measurements were taken at depths of 0.5 m, 1.0 m and 1.5 m using a GSI Ltd designed K-type digital temperature probe incorporating a quick response tip. In 2012, 29 sites were measured. In 2023, nine of these sites were measured again, with the other 20 sites being inaccessible. Seventeen new sites were measured in 2023; (2) Surface temperature measurements were obtained at the start and end points of 13 repeated GPR transects and seven new 2023 GPR transects. Equipment used was a digital temperature probe with a K-type thermocouple.

The ambient air temperatures in 2012 and 2023 was 10.8 °C (9am) and 18 °C (3pm), respectively.

3. RESULTS

3.1 Temperature Measurements

3.1.1 Subsurface Temperatures

The 2012 and 2023 downhole temperature measurements are given in Table 1. Figures 3 and 4 show the location of these measurements with measured temperatures separated into temperature groups. Some of the 2023 measurement sites have a different number to the 2012 sites.

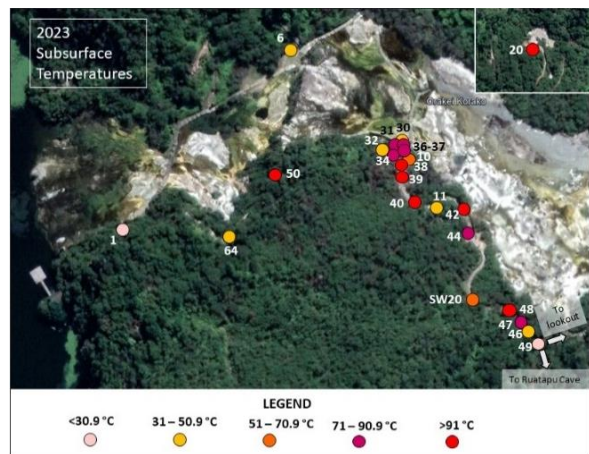


Figure 3: 2023 downhole temperatures measurement sites with corresponding temperature groups shown. Insert: Mud pools.

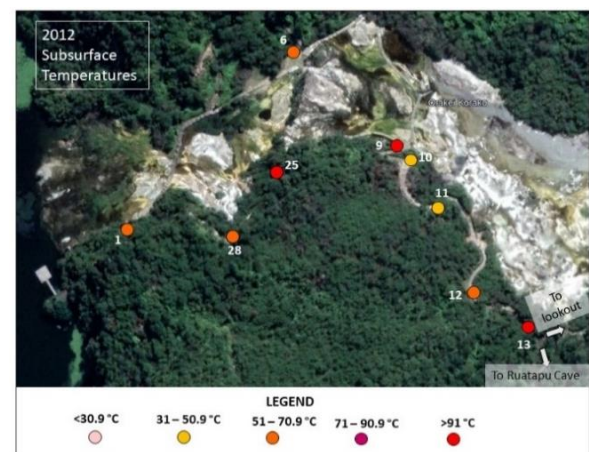


Figure 4: 2012 downhole temperatures measurement sites that match the 2023 downhole temperature measurement sites. Temperature groups shown.

Our survey revealed that one area has had minimal temperature change (little cave before Soda Fountain), three areas have decreased in temperature (boardwalk by Diamond Geyser, grassed area by Devil's Throat, and the boardwalk west of fossilised outcrop by Wairiri Geyser) and five areas have increased in temperature (mud pools, Soda Fountain area and three areas between the viewing platform overlooking Wairiri Geyser and the turn off to Artist's Palette viewing platform; Fig. 5).

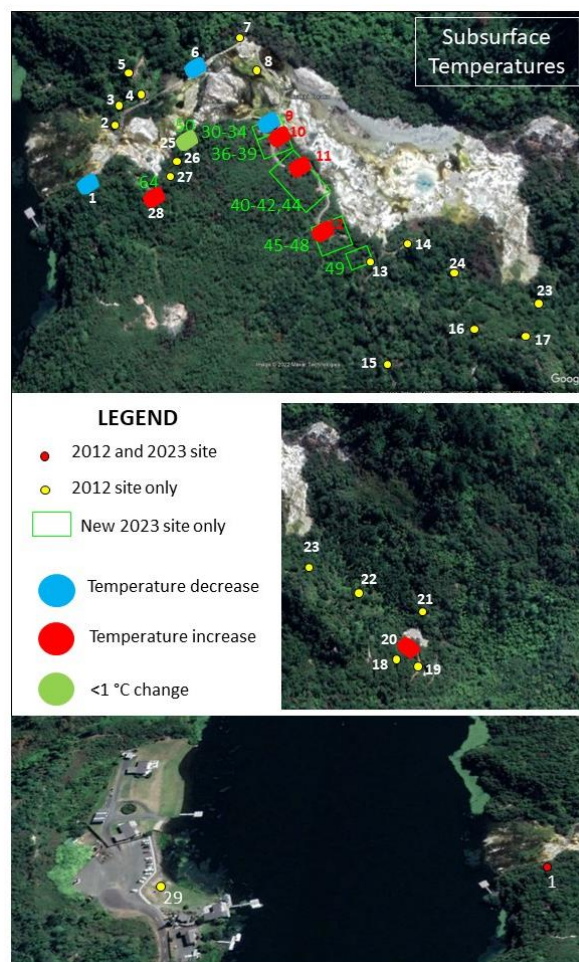


Figure 5: Map showing where and how the shallow subsurface temperatures have changed between 2012 and 2023 at the nine sites where their locations could be matched.

Table 1: Shallow subsurface temperatures for the nine locations that were measured in 2012 and 2023.

2012 site number	Depth (m)	Temperature (°C)
2023 site number		
1	<0.5	51.8
1	0.1	20.4
6	1.5	77.1
6	1.5	50.8
9	<0.5	100
31	0.05	89.6
10	<0.5	30.1
10	0.2	68
11	<0.5	41.2
11	0.3	44.8
12	<0.5	58
44	surface	78
20	1.5	73.3
20	1.2	99.8
25	<0.5	99.4
50	0.5	99.6
28	<0.5	45
64	0.2	41.1

3.1.1 Surface Temperatures

Ten 2023 GPR transects were repeated at the same locations as the 2012 transect lines. The surface temperature at the start and end of both the 2012 and 2023 GPR transect line was measured for comparison (Table 2).

Table 2: Temperature readings at start and end of each GPR transect in 2012 and 2023. T = temperature.

Profile 2012 2023	GPR length (m)	2012 T at start 2023 T at start (°C)	2012 T at end 2023 T at end (°C)
G1 SW6	10 10	33.4 18.5	18.2 18.4
G2 SW8	12 12	21.7 23.5	- 32.2
G3 SW9	21 21	15.2 21.9	14.5 36.9
G4 SW11	5 5	15.6 22.3	22.2 22.8
G5 SW10	5 5	16.4 24.2	20.6 24.6
G6 SW12	10 10	18.2 18.0	13.9 22.5
G7 SW13	10 10	15.3 18.0	11.6 20.8
G9 SW15	13 13	39.1 33.8	31.0 21.8
G14 SW19	18.4 18.4	20.0 27.7	17.9 37.2
G18 SW24	10 10	9.6 19.0	- 16.0

Our results show that some sites have increased, while other sites have decreased in surface temperature over the last 11 years (Fig. 6). The areas that revealed an increase in surface temperature are; the boardwalk across Emerald/Rainbow Terrace, (G2 on Fig. 6), the northern lookout area (G4 on Fig. 6), two areas on the northern side of Devil's Throat (G3, G5-7 on Fig. 6), Elephant Rock (G14 on Fig. 6), the entrance to Ruatapu Cave (G18 on Fig. 6). Two areas that have decreased in temperature are; the boardwalk by Diamond Geyser (G1 on Fig. 6) and the new boardwalk west of Wairiri Geyser (G9 on Fig. 6).

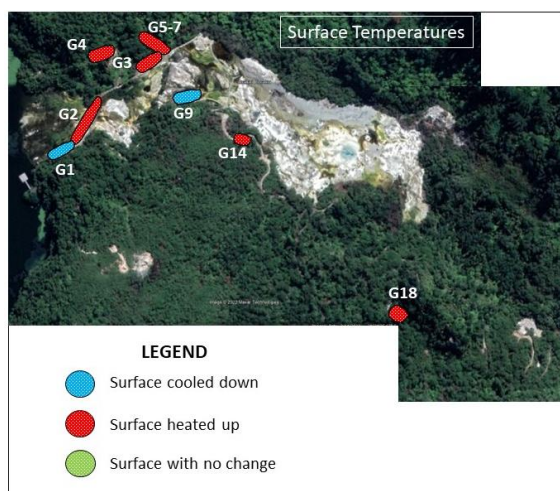


Figure 6: Map showing locations where the surface temperature has either increased, decreased or remained unchanged between 2012 and 2023.

3.2 Ground Penetrating Radar

The location of the 2012 and 2023 GPR sites are presented in Figure 7, with the direction of the GPR data collection indicated by the line from the square. Our GPR survey mapped fractures, identified locations of steam conduits and enabled the thickness of the sinter terraces to be estimated. Figures 8 to 13 have been chosen to represent a range of findings made in this study.

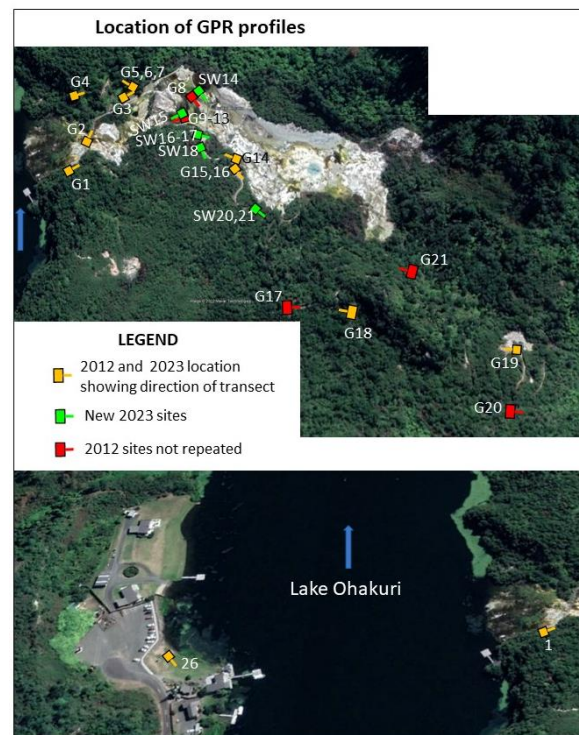


Figure 7: Map showing the location of the 2023 and 2012 GPR sites. Blue arrow indicates the flow direction of the Waikato River at Lake Ohakuri.

3.2.1 Shallow steam vents and sinter thickness

Two new 2023 GPR profiles (SW16 and SW17) were captured on the viewing platform that overlooks Wairiri Geyser and lies directly over a historic sinter outcrop (Fig. 8).

Figure 9 shows our GPR results for transects SW16 and SW17. At the start of transect SW16, the surface temperature measured 37 °C which correlates to moderate-weak reflections. At the 2 m mark, the temperature increased to 68 °C and this area shows weak reflections. The decrease in the GPR signal strength correlates directly to an increase in temperature. At the 3.7 m mark, the surface temperature measured 90 °C, directly over a small vent. Temperatures surrounding the vent were between 70-80 °C. The 90 °C vent is above the strong amplitude reflections suggesting either: (1) This area is newly-heated and the underlying sinter has not had enough time to become sufficiently altered, which would produce weak reflections; or (2) The unaltered sinter (strong reflections) are creating a barrier and the steam is ascending alongside the strong amplitude reflection area.

Strong reflections are detected to 6 m depth suggesting the sinter here is 6 m thick. Sinter exposed in the outcrop beneath this GPR transect line is ~2.5 m thick.



Figure 8: Site photographs of transect locations SW16 and SW17, with measured surface temperatures.

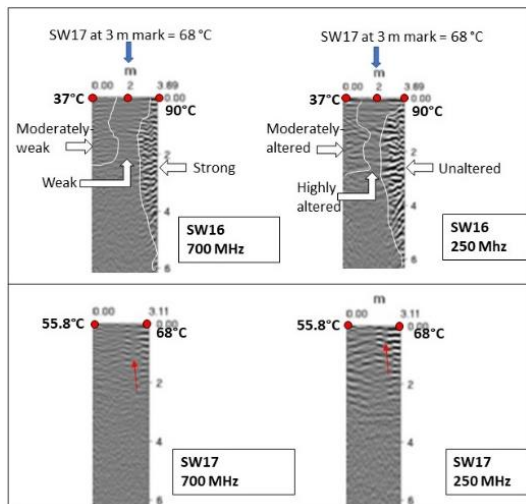


Figure 9: GPR profiles for SW16 and SW17. Surface temperature measurements given. For SW16, moderately-weak reflections occur between 0 and 1.5 m, weak reflections between 1.5 to 3 m and strong reflections from 2.8 and 3.6 m occur down to 6 m depth. For the SW17 profile, vertical conduits of weak reflections (red arrows) are separated by moderate and strong reflections.

3.3.2 Fractures, steam conduits and sinter thickness

In 2012, GPR site G8 could not be repeated due to microbial mats covering the sinter surface. A new GPR profile (SW14) was collected parallel to site G8 along the boardwalk on Golden Fleece Terrace. The two transects were located ~5 m apart (Fig. 10A-B).

The 2012 GPR image (Fig. 10C) shows three vertical bands of weak reflections to a depth of 3 m, separated by moderate reflections. One of the 2012 vertical weak reflection bands correlated to a measured temperatures of 92.1 °C at 1.5 m depth, confirming heat in the subsurface in 2012 (Fig. 10C). These weak amplitude vertical conduits represent pathways where steam is ascending and hydrothermal alteration of the sinter was actively taking place in 2012.

The vertical bands of weak reflections present in 2012 at the 1 and 2 m marks, do not appear in the 2023 GPR profile, located 5 m away. However, the third vertical band of weak reflections present in 2012, at the 4-5 m mark, does correlate to a change from strong to moderately-strong reflections in 2023 image (Fig. 10D-E). Although the two GPR transects are 5 m apart, there may be a fracture between the GPR transect lines at the 4 m mark, although the alteration of the sinter caused by the ascending steam is more intense in the 2012 profile line (Fig. 10F).

Offsets in the GPR reflections at ~5.8 m along the 2023 GPR transect line suggest a subsurface fracture to at least 2 m depth (Fig. 10E). No strong reflections were observed in 2012, but they are visible, in patches along the 2023 GPR profile line. These indicate unaltered sinter with a maximum thickness of 2 m (Fig. 10E).

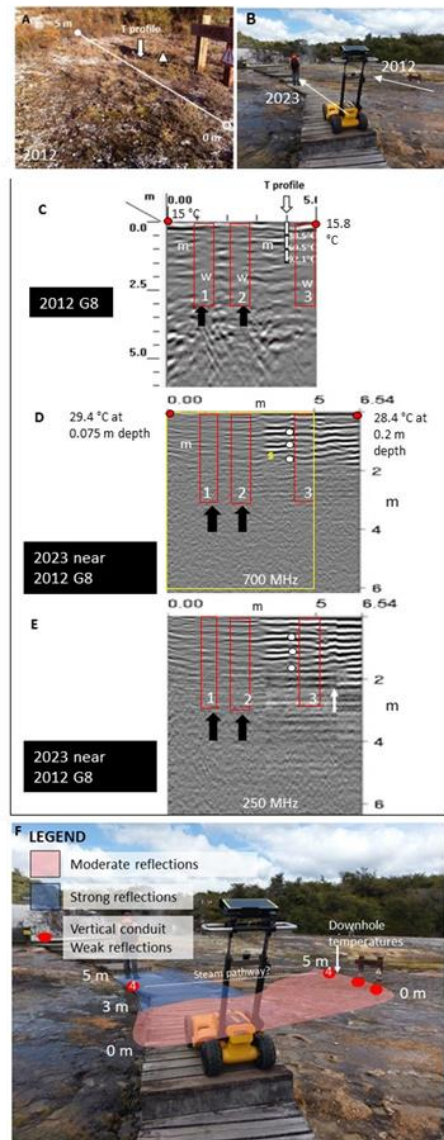


Figure 10: Site G8/SW14. (A-B) Location of the 2012 and 2023 GPR profiles. (C) 2012 GPR image. Red boxes show change in strength of GPR reflections from moderate (m) to weak (w). Surface and downhole temperatures shown. (D-E) 2023 GPR images. Red boxes 1-3 correlate to the red boxes in (A), where moderate (m) reflections are visible inside and surrounding boxes 1 and 2. Inside box 3 moderately-strong reflections surrounded by strong reflections. White circles indicate corresponding depths and locations of the 2012 downhole temperature measurements. Fracture (arrow) at ~5.8 m. Measured temperatures shown. Yellow box represents area scanned in 2012. (F) Relationship of 2012 and 2023 GPR reflections to site photograph.

3.3.3 Increased heat in subsurface between 2012 and 2023

An example of our repeat survey showing a heat increase in the shallow subsurface over the last 11 years is shown at GPR site G19 (Fig. 11). At the 8 m mark along both the 2012 and 2023 GPR transect lines, the measured temperature at 1.5 m depth has increased from 73.3 to 99.8 °C, in 2012 and 2023, respectively. Although the subsurface temperature has increased, moderate amplitude reflections are observed. This suggests that this area is newly heating up, as if the 99.8 °C had been sustained for a significant period of time, weak amplitude reflections would be expected.

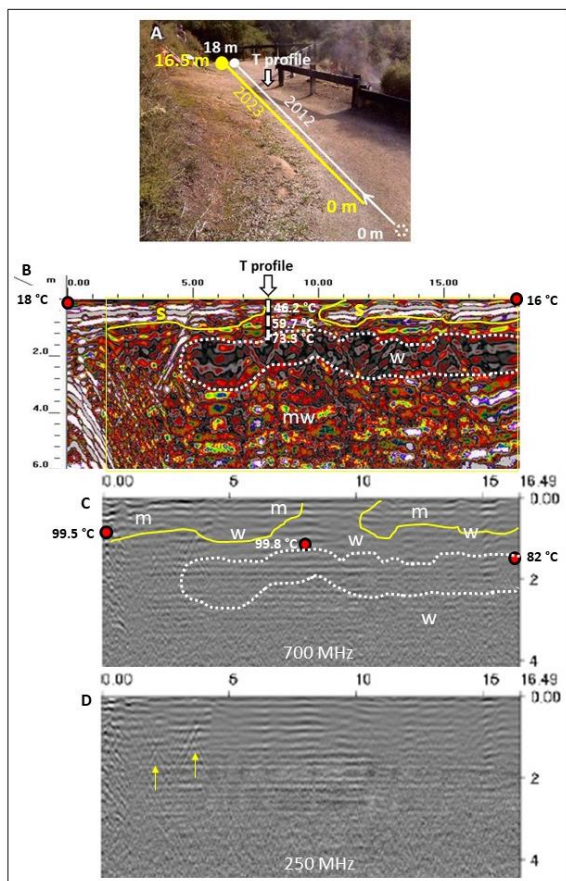


Figure 11: GPR site G19. (A) Site photograph. (B) 2012 GPR image with strong (s), moderate (m) and weak (w) reflections. Downhole temperature measurements shown. (C-D) 2023 GPR image with moderate (m) and weak (w) amplitude reflections shown. Temperature measurements given. Yellow arrows indicate hyperbolas.

3.3.4 2019 new vents

The 2012 GPR profile could not be repeated as the boardwalk has been moved several metres to the north, due to the appearance of three vents, in 2019. The 2023 GPR profile runs parallel to the 2012 GPR profile, along the new boardwalk (Fig. 12). Although site G9 is located several metres to the north of the 2019 vents, (i) distinctive vertical conduits of weak amplitude reflections are visible in the 2023 GPR image, below the new vents, and (ii) strong reflections are visible in the 2023 images that line up with the sides of the new vents, but several metres to the north of the vents.



Figure 12: Sites G9 (2012) and SW15 (2023). (A) Overview of the 2012 site G9. (B) The new vents in 2019 and the new boardwalk. (C) Relationship between 2012 and 2023 GPR profiles shown.

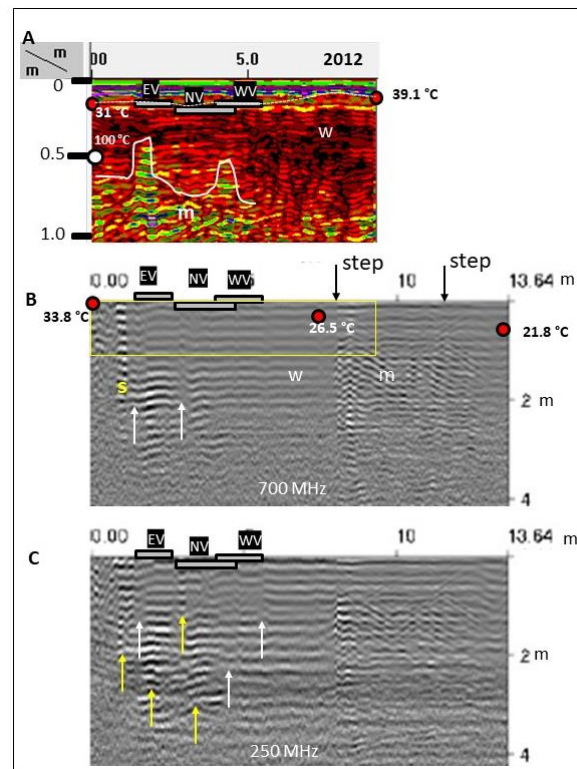


Figure 13: GPR profiles of the 2012, G9 site, and the 2023, SW15 site. Location of the East vent (EV), North vent (NV) and West vent (WV) are shown. (A)

2012 GPR image with areas of moderate (m) and weak (w) reflections. Sinter surface below boardwalk shown as white dotted line. Measured temperatures at both ends of the transects are shown. (B-C) 2023 GPR images show vertical bands of strong reflections parallel (yellow arrows) to the sides and beneath the East and North vents. White arrows indicate vertical zones of weak reflections that line up with the three vents, although several metres to the North. Yellow box in (B) indicates area scanned in 2012.

3.3.5 GPR Summary

Figure 14 summarises the GPR finding of our 2012 and 2023 surveys. Some GPR transect lines revealed no change while others imaged steam conduits and/or fractures that were either present in both surveys or present in either only 2012 or 2023. Four locations where the GPR profile was directly over a sinter terrace showed strong reflections, suggesting unaltered sinter. These GPR images mapped varying sinter thicknesses at each site from one to three metres thick.

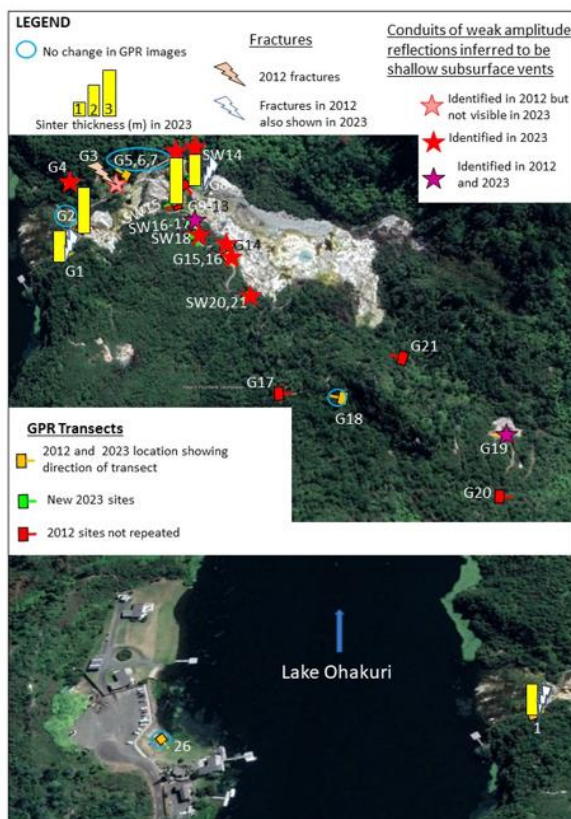


Figure 14: Summary of changes detected by GPR between 2012 and 2023.

3.4 CONCLUSIONS

A Ground Penetrating Radar (GPR) and downhole temperature survey around the boardwalk at Orakei Korako geothermal field was completed in March 2023. This survey was a repeat of a 2012 survey. The purpose of the repeat survey was to image the subsurface and identify if any changes had taken place in the last 11 years.

Nine 2012 downhole temperature measurement sites and ten surface temperature measurements sites were repeated for a direct comparison with our 2023 data. Thirteen GPR sites were repeated in 2023, five 2012 GPR sites were not repeated

due to inaccessibility to the site. GPR profiles from seven new sites were also collected during the 2023 survey.

Key findings include:

- Surface and subsurface temperatures have increased by 10-40 °C in the Elephant Rock area.
- The shallow subsurface immediately West of Wairiri Geyser, by the stairs going up to the viewing platform, has cooled by 10 °C but remains hot at 89 °C. The surface temperatures have also cooled by ~5 °C with maximum measured temperatures now 34 °C.
- The area north of Devil's Throat has cooled in the subsurface from 77 °C to 51 °C but has increased at the surface from 14-15 °C to 22-37 °C.
- Surface temperatures have increased in the mud pools area, along the path between the Wairiri Geyser lookout and the turn-off to the Artist's Palette lookout and by Soda Fountain.
- Surface temperatures have increased in the northern part of the boardwalk.
- GPR documented the sinter thickness at several locations.
- The dual technique of GPR and downhole temperature measurements tracked locations of heat in the shallow subsurface, even when there was no evidence of heat at the surface.
- Repeated GPR surveys combined with downhole temperature surveys enabled the tracking of heat migration pathways in the shallow subsurface. This is important for the evaluation of whether localised areas are heating up or cooling down.
- Currently active and historic zones of hydrothermal alteration were identified and mapped.
- The 2012 survey mapped fracture locations, and the 2023 survey confirmed if they were still present, and mapped the appearance of new fractures.

ACKNOWLEDGEMENTS

We would like to thank Waikato Regional Council, especially Katherine Luketina for supporting this project and the staff at Orakei Korako for allowing unlimited access to the site.

REFERENCES

- Campbell, K.A., Sannazzaro, K., Rodgers, K.A., Herdianita, N. R., Browne, P.R.L., (2001). Sedimentary Facies and Mineralogy of the Late Pleistocene Umukuri Silica Sinter, Taupo Volcanic Zone, New Zealand. *Journal of Sedimentary Research*, 71(5), 727–746.
- Campbell, K., Lynne, B., Handley, K., Jordan, S., Farmer, J., Guido, D., Foucher, F., Turner, S., Perry, R., (2015). Tracing Biosignature Preservation of Geothermally Silicified Microbial Textures into the Geological Record. *Astrobiology*, 15, 858–882.
- Dougherty, A., Lynne, B.: A novel geophysical approach to imaging sinter deposits and other subsurface geothermal features utilizing ground penetrating radar. *Geothermal Resource Council Transactions*, 34, pp. 787–791. (2010a).
- Dougherty, A., Lynne, B.Y.: Finding vents and fractures in geothermal systems using Ground Penetrating Radar.

Proc. 32nd New Zealand Geothermal Workshop, New Zealand. (2010b).

Dougherty, A., Lynne, B.: Utilizing ground penetrating radar and infrared thermography to image vents and fractures in geothermal environments. *Geothermal Resource Council Transactions*, 35, pp. 743–749. (2011).

Foley, D., Lynne, B.Y., Jaworowski, C., Heasler, H., Smith, G., Smith, I.: Ground Penetrating Radar Investigation of Sinter Deposits at Old Faithful Geyser and Immediately Adjacent Hydrothermal Features, Yellowstone National Park, Wyoming, USA. *AGU Fall Meeting*, San Francisco, USA. (2015).

Fournier, R.O., Rowe, J.J. (1966). Estimation of underground temperatures from the silica content of water from hot springs and wet-steam wells. *American Journal of Science*, 264(9), 685–697.

Fournier, R.O. (1985). The Behavior of Silica in Hydrothermal Solutions. In: Berger, B.R., Bethke, P. M. (Eds.), *Geology and Geochemistry of Epithermal Systems* (2). *Society of Economic Geologists*.

Jaworowski, C., Lynne, B.Y., Heasler, H., Foley, D., Smith, I.J., Smith, G.J. (2020). Detecting natural fractures with ground penetrating radar and airborne night-thermal infrared imagery around Old Faithful Geyser, Yellowstone National Park, USA. *Geothermics*, 85, 101775.

Lynne, B., Campbell, K., Moore, J.N., Browne, P.R.L. (2005). Diagenesis of 1900-year-old siliceous sinter (opal-A to quartz) at Opal Mound, Roosevelt Hot Springs, Utah, U.S.A. *Sedimentary Geology*, 179, 249–278.

Lynne, B.Y., Campbell, K.A., Moore, J., Browne, P.R.L. (2008). Origin and evolution of the Steamboat Springs siliceous sinter deposit, Nevada, U.S.A. *Sedimentary Geology*, 210(3), 111–131.

Lynne, B., Dougherty, A.: Ground Penetrating Radar Successful in Imaging Hot Spring Deposits: A New Geothermal Exploration Tool. *AGU Fall Meeting Abstracts*. (2010a).

Lynne, B.Y., Dougherty, A.: Mapping the spatial extent of buried hot spring deposits in New Zealand and the USA using Ground Penetrating Radar. *GeoNZ 2010 Conference, Miscellaneous Publication 129A*. (2010b).

Lynne, B.Y., Smith, G.J.: Tracking fluid flow migration pathways at Orakei Korako, New Zealand. *Proc. 36th New Zealand Geothermal Workshop. New Zealand*. (2014).

Lynne, B.Y., Smith, I.J., Smith, G.J., Luketina, K.: Imaging the Shallow Subsurface of Armstrong Reserve, Taupo. *Proc. 38th New Zealand Geothermal Workshop, Auckland, New Zealand*. (2016).

Lynne, B.Y., Heasler, H., Jaworowski, C., Smith, I.J., Smith, G.J., Foley, D.: Ground Penetrating Radar Imaging of Old Faithful Geyser Vent, Yellowstone National Park, USA. *Proc. 38th New Zealand Geothermal Workshop, Auckland, New Zealand*. (2016b).

Lynne, B., Smith, G.J., Heasler, H., Jaworowski, C., Smith, I.J., Foley, D., Sahdarani, D.: Post depositional alteration of siliceous sinter near Old Faithful Geyser, Yellowstone National Park, USA. *Geothermal Resource Council Transactions*. (2017).

Lynne, B.Y., Smith, G.J., Heasler, H., Jaworowski, C., Smith, I.J., Foley, D.: Tracking Shallow Hydrological Changes in Micro-Fractured Siliceous Sinter During Pre-eruptive Cycles Of Old Faithful Geyser Vent, Yellowstone National Park, USA. *Geothermal Resource Council Transactions*. (2018).

Williams, L.A., Crerar, D.A. (1985). Silica Diagenesis, II: general mechanisms. *Journal of Sedimentary Petrology*, 55, 312–321.